JRC Scientific and Technical Reports

Geometric Quality Testing of the Kompsat-2 Image Data Acquired over the JRC Maussane Test Site using ERDAS LPS and PCI GEOMATICS remote sensing software

Joanna Krystyna Nowak Da Costa
Agnieszka Walczyńska

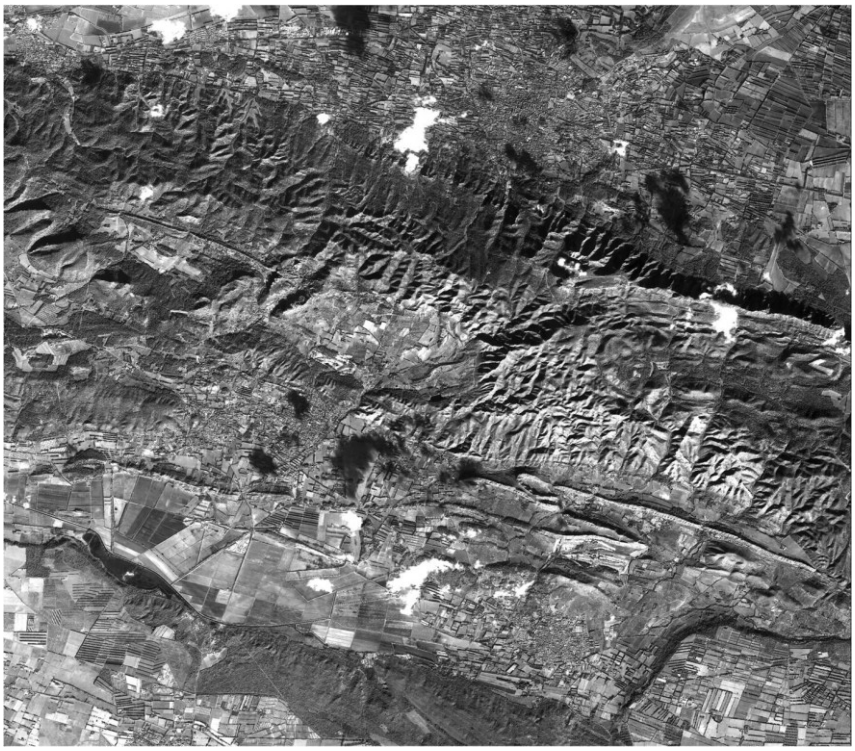

EUR 24542 EN - 2010

JRC
EUROPEAN COMMISSION

ipsc
Institute for the Protection and Security of the Citizen

The mission of the JRC-IPSC is to provide research results and to support EU policy-makers in their effort towards global security and towards protection of European citizens from accidents, deliberate attacks, fraud and illegal actions against EU policies.

European Commission
Joint Research Centre
Institute for the Protection and Security of the Citizen

Contact information
Address: T.P. 266, Via E. Fermi 2749, I-21027 Ispra (VA), Italy
E-mail: joanna.nowak@jrc.ec.europa.eu
Tel.: +39 0332 78 5854
Fax: +39 0332 78 9029

http://ipsc.jrc.ec.europa.eu/
http://www.jrc.ec.europa.eu/

JRC 60285

EUR 24542 EN
ISBN 978-92-79-17007-2
ISSN 1018-5593
doi:10.2788/21463

Luxembourg: Publications Office of the European Union

Printed in Italy

Table of Contents

1. Objective

This report summarizes the outcome of the geometric quality testing of the Kompsat-2 (K2) images acquired over the JRC Maussane Terrestrial Test Site.

The objective of this study is threefold:

(1) to evaluate the planimetric accuracy in a routine basis production of orthorectified Kompsat-2 imagery;

(2) to determine the optimal number and spatial distribution of the GCPs (Ground Control Points) for the Kompsat-2 orthorectification process;

(3) to check if the orthorectified imagery of the Kompsat-2 optical sensor fall within the required accuracy criteria for the CwRS 1:10.000 scale of absolute 1-D RMSE of < 2.5m.

2. Data description

2.1. Kompsat-2 satellite and image data

KOMPSAT-2 (KOrean MultiPurpose SATellite) is the very-high-resolution satellite was developed by the (South) Korean Aerospace Research Institute (KARI). It was successfully launched on July 28, 2006 by a Rockot launch vehicle at the Plesetsk Cosmodrome in northern Russia. It weighs 800 kg and has 1,000 watts of power and is operating at the same orbital altitude of KOMPSAT-1 (source: http://www.kari.re.kr/english/, http://www.spotimage.com).

The KOMPSAT-2 allows for generation of high resolution images with a GSD of better than 1 m for PAN data and 4 m for MS data with nadir viewing condition at the nominal altitude of 685 km. The MSC has a single PAN spectral band between 500 - 900 nm and 4 MS spectral bands between 450-900 nm. PAN imaging and MS imaging can be operated simultaneously during mission operations. The swath width is greater than or equal to 15 km at the mission altitude for PAN data and MS data. The system is equipped with a solid state recorder to record images not less than 1,000km long at the end of life (KOMPSAT-2 Image Data Manual, 2008).

The satellite can be rolled up to ±30 degrees off-nadir to pre-position the MSC swath. The KOMPSAT-2 can provide across-track stereo images by multiple passes of the satellite using off-nadir pointing capability. The satellite is compatible with daily revisit operation by off-nadir pointing with degraded GSD.

Orbital elements	
Orbit type	Near polar, Sun synchronous
Altitude	685.13 km
Inclination	98.127° (Sun synchronous)
Orbital per day	28
Revisit rate	3 days
Instruments	
Payload	B&W (PAN) and 4 MS (R, V, B, PIR)
Spectral band	PAN: 500nm - 900nm MS1 (Green): 520nm - 600nm MS2 (Blue): 450nm - 520nm MS3 (NIR): 760nm - 900nm MS4 (Red): 630nm - 690nm
Spatial resolution	1 m (PAN) and 4m (MS) at nadir
Radiometric resolution	10 bits/pixel (delivery 16bits/pixel)
Swath (footprint)	15 km x15 km
Viewing angle	±30° (roll/pitch tilt)

Table 1: Kompsat-2 parameters (KOMPSAT-2 Image Data Manual, 2008)

2.2. Processing Level Definitions of Kompsat-2 image data product

Level 0 data is the received and stored image data within which any and all communications artifacts (e.g. synchronization frames, communications headers) are removed.

Level 1A data is a processed image data at full resolution, time-referenced, and annotated with ancillary information, including radiometric and geometric calibration coefficients and georeferencing parameters (i.e., platform ephemeris) computed and appended to the Level 0 data, and catalogued by KGRS-2, corrected by the MSC image restoration, cloud cover assessed (CCA) and stored by raw format with imagery data and ASCII format with ancillary data (KOMPSAT-2 Image Data Manual, 2008).

Level 1R data is the image data cut by catalogue (15000 column X15500 line), optionally MTF corrected and stored by Tiff format. Generally, the remote sensing satellite image data is radiometrically corrected in the processing step of Level 1R. However for the MSC image data it is not, because MSC image data is already radiometrically corrected by the NUC (Non-Uniformity Correction) within the MSC. If user wants, MTFC (MTF correction or MTF compensation) is applied to the Level 1R image data optionally.

Level 1G data is geometrically corrected from Level 1R image data using KOMPSAT-2 ancillary data only and stored by GeoTiff format. Level 1G data projected onto ellipsoid (h=0), map oriented and terrain displacement. If user wants, MTFC (MTF correction or MTF compensation) will be applied to the Level 1R image data optionally (KOMPSAT-2 Image Data Manual, 2008).

2.3. Nominal geo-location accuracy of Kompsat-2 sensor image

According to Seo (2008) from Korea Aerospace Research Institute (KARI) 'the horizontal geo-location accuracy of KOMPSAT-2, without GCPs (Ground Control Points) is 80 meters CE90 for monoscopic image of up to 26 degrees off-nadir angle, after processing including POD (Precise Orbit Determination), PAD(Precise Attitude Determination) and AOCS (Attitude and Orbit Control Subsystem) sensor calibration. In case of multiple stereo images, without GCPs, the vertical geometric accuracy is less than 22.4 meters LE 90 and the horizontal geometric accuracy is less than 25.4 meters.'

Horizontal accuracy CE90 of 80m corresponds to the horizontal (2-D) RMS error of 40.8m.

Saunier (2008) in his Kompsat-2 Mission Quality Assessment refers to 1R product geo-location as follows:

		Multi Spectral	Panchromatic (PAN)	PAN with one GCP
Product ID 4340 (1R)	RMSE Easting [m]	10.7	11.8	5.3
	RMSE Northing [m]	35.4	37.7	4.0
Product ID 5114 (1R)	RMSE Easting [m]	n/a	33.7	4.6
	RMSE Northing [m]	n/a	23.2	4.6

Furthermore, in his 'Ortho Product Testing – Kompsat-2 (2008), GAEL reports the Kompsat-2 1R geo-referencing quality using RPC-based modeling method based on eight (8) ground control points (table below). In the same table one can find the the geometric quality results of the orthorecified image based on eight independent check points.

Product ID 128-1325 (1R)	Geo-referred PAN using 8 GCPs	ORTHO PAN using 8 GCPs, validated using 8 ICPs
RMSE_Easting [m]	2.8	2.8
RMSE_Northing [m]	5.1	5.9

2.4. Study area and Kompsat-2 data for testing

The MARS Unit was provided with four samples of Kompsat-2 image product, level 1R. The image GeoTIFF files are accompanied by image support data, i.e. metadata file and RPC file, in the simple ASCII format. The basic characteristics of our K2 images are as follows (Table 2):

Image ID number	MSC_100202092609 _18772_ 01251327PP13_1R	MSC_100118093842 _18553_ 01251327PP29_1R	MSC_071007094533 _06370_ 01251328PN12_1R	MSC_090128093655 _13367_ 01251328PN00_1R
Image short ID	**1**	**2**	**3**	**4**
Image product level	1R	1R	1R	1R
Acquisition Date	02 February 2010, 09:26	18 January 2010, 09:38	07 October 2007, 09:45	28 January 2009, 09:36
Tilt angle ROLL (rotation about the in-track direction) Across-Track Angle	13.9 deg	29.6 deg	-12.6 deg	-0.4 deg
Tilt angle PITCH (rotation about the cross-track direction) In-Track Angle	0.3 deg	0.7 deg	-0.7 deg	-0.3 deg
Satellite Azimuth	255.8 deg	260.2 deg	-20.9 deg	58.7 deg
Incidence Angle	15.5 deg	33.3 deg	75.9 deg	1.3 deg
GSD Along Track	1.044 m	1.394 m	1.394 m	0.982 m
GSD Across Track	1.014 m	1.151 m	1.151 m	0.996 m
Map Projection	UTM: North, 31 WGS 84			
Ellipsoid, Datum	WGS 84			
Off-nadir	13.9 deg	29.6 deg	12.6 deg	1 deg

Table 2: Basic metadata of the Kompsat-2 sample images (according to image provider metadata file)

The JRC Maussane Terrestrial Test site is located near to Mausanne-les-Alpilles in France. It has been used as test site by the European Commission Joint Research Centre since 1997. It comprises a time series of reference data (i.e. DEMs, imagery, and ground control) and presents a variety of agricultural conditions typical for the EU. The site contains a low mountain massif (elevation up to around 650m above sea level), mostly covered by forest, surrounded by low lying agricultural plains and a lot of olive groves. A number of low density small urban settlements and a few limited water bodies are present over the site.

The location of the sample K2 images over our test site is presented in Fig.1.

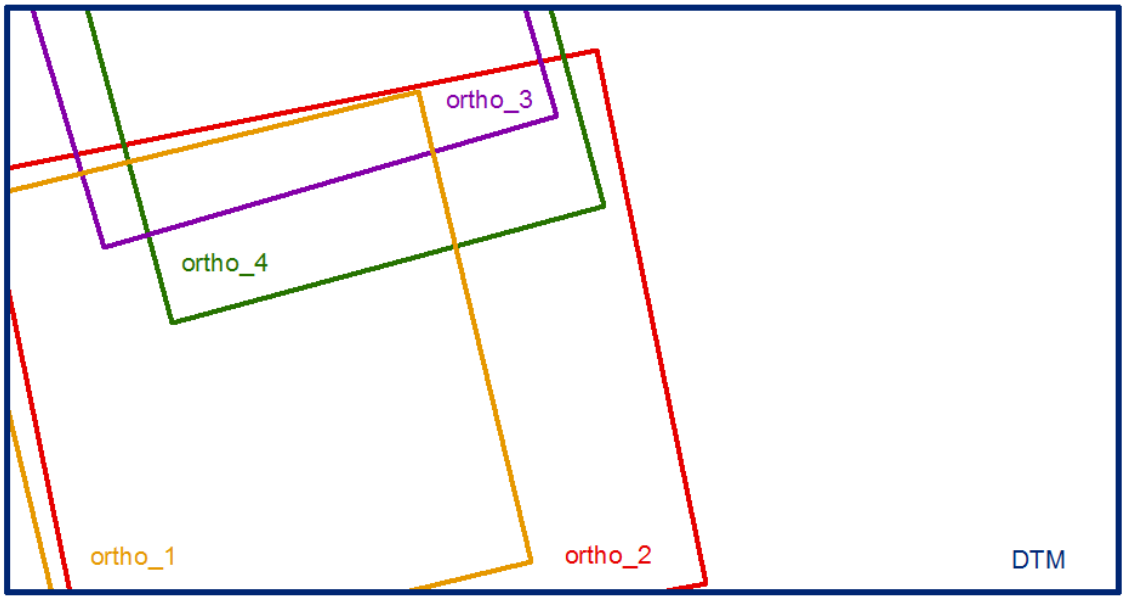

Figure 1: The location of the Kompsat-2 sample orthoimages and the JRC Maussane Test Site limited by very accurate (0.6m RMSEz) Digital Terrain Model (DTM).

2.5. Auxiliary Data

The following auxiliary data was used during sensor orientation and orthorectification of the Kompsat-2 image ID1:

- Set of 2 GCPs from the ADS40 project: RMSEx < 0.05m; RMSEy = 0.10m (110002, 110008);
- Set of 1 GCPs from the VEXEL project: RMSEx = 0.49m; RMSEy = 0.50m (440008);
- Set of 1 GCPs from the Cartosat-2 project RMSEx = 0.90m; RMSEy = 0.76m (G7001)
- Set of 1 GCPs from the multi-use project RMSEx = 0.30m; RMSEy = 0.30m (66035);
- Set of 10 GCPs chosen and measured on the aerial ADS40 ortho: RMSEx = 0.90m; RMSEy = 0.76m (990045, 990046, 990047, 990048, 990049, 990050, 990051, 990052, 990053, 990054);
- DEM_ ADS40 – digital elevation model generated from ADS40 (Leica Geosystems) digital airborne image with 2m resolution and RMSEz=0.6m.

The following auxiliary data was used during sensor orientation and orthorectification of the Kompsat-2 image ID2:

- Set of 2 GCPs from the ADS40 project: RMSEx < 0.05m; RMSEy = 0.10m (110008, 110038);
- Set of 1 GCPs from the VEXEL project: RMSEx = 0.49m; RMSEy = 0.50m (440008);
- Set of 1 GCPs from the Cartosat-2 project RMSEx = 0.90m; RMSEy = 0.76m (G7001);
- Set of 1 GCPs from the multi-use project RMSEx = 0.30m; RMSEy = 0.30m (66035);
- Set of 10 GCPs chosen and measured on the aerial ADS40 ortho: RMSEx = 0.90m; RMSEy = 0.76m (990026, 990035, 990036, 990037, 990038, 990039, 990040, 990041, 990042, 990043);

- DEM_ ADS40 – digital elevation model generated from ADS40 (Leica Geosystems) digital airborne image with 2m resolution and RMSEz=0.6m.

The following auxiliary data was used during sensor orientation and orthorectification of the Kompsat-2 image ID3:

- Set of 12 GCPs chosen and measured on the aerial ADS40 ortho: RMSEx = 0.90m; RMSEy = 0.76m (990049, 990055, 990056, 990057, 990058, 990059, 990060, 990061, 990062, 990063, 990054, 990064);
- DEM_ ADS40 – digital elevation model generated from ADS40 (Leica Geosystems) digital airborne image with 2m resolution and RMSEz=0.6m.

The following auxiliary data was used during sensor orientation and orthorectification of the Kompsat-2 image ID4:

- Set of 1 GCPs from the Cartosat-2 project RMSEx = 0.90m; RMSEy = 0.76m (G7003);
- Set of 11 GCPs chosen and measured on the aerial ADS40 ortho: RMSEx = 0.90m; RMSEy = 0.76m (990008, 990049, 990056, 990057, 990058, 990062, 990072, 990073, 990075, 990076, 990080);
- DEM_ ADS40 – digital elevation model generated from ADS40 (Leica Geosystems) digital airborne image with 2m resolution and RMSEz=0.6m.

The projection and datum details of the above listed data are UTM zone 31N ellipsoid WGS84.

2.6. Validation Data

The points with known position that were not used during the used during the geometric correction model phase served as the validation sets[1] in order to evaluate planimetric error of the test orthoimage data.

The ICP control set for the Kompsat-2 image ID1 consisted of the following 15 points:

- Set of 1 ICPs from the ADS40 project: RMSEx < 0.05m; RMSEy = 0.10m (110021);
- Set of 1 ICPs from the VEXEL project: RMSEx = 0.49m; RMSEy = 0.50m (440024);
- Set of 1 ICPs from the Cartosat-2 project RMSEx = 0.90m; RMSEy = 0.76m (G7023);
- Set of 1 ICPs from the Formosat-2 project RMSEx = 0.88m; RMSEy = 0.72m (550011);
- Set of 3 ICPs from multi-use project RMSEx = 0.30m; RMSEy = 0.30m (66014, 66022, 66023);
- Set of 8 GCPs chosen and measured on the aerial ADS40 ortho: RMSEx = 0.90m; RMSEy = 0.76m (990003,990005, 990008, 990019, 990022, 990024, 990032, 990044);

The ICP control set for the Kompsat-2 image ID2 consisted of the following 15 points:

- Set of 1 ICPs from the ADS40 project: RMSEx < 0.05m; RMSEy = 0.10m (110021);

[1] also referred as to independent control points (ICPs)

- Set of 1 ICPs from the VEXEL project: RMSEx = 0.49m; RMSEy = 0.50m (440024);
- Set of 1 ICPs from the Cartosat-2 project RMSEx = 0.90m; RMSEy = 0.76m (G7023);
- Set of 1 ICPs from the Formosat-2 project RMSEx = 0.88m; RMSEy = 0.72m (550011);
- Set of 3 ICPs from the multi-use project RMSEx = 0.30m; RMSEy = 0.30m (66014, 66022, 66023);
- Set of 12 ICPs chosen and measured on the aerial ADS40 ortho: RMSEx = 0.90m; RMSEy = 0.76m (990003,990005, 990008, 990019, 990022, 990024, 990032, 990044);

The ICP control set for the Kompsat-2 image ID3 consisted of the following 10 points:

- Set of 1 ICPs from the ADS40 project: RMSEx < 0.05m; RMSEy = 0.10m (110010);
- Set of 2 ICPs from the Cartosat-2 project RMSEx = 0.90m; RMSEy = 0.76m (G7001, G7010);
- Set of 7 ICPs chosen and measured on the aerial ADS40 ortho: RMSEx = 0.90m; RMSEy = 0.76m (990065, 990066, 990067, 990068, 990069, 990070, 990071);

The ICP control set for the Kompsat-2 image ID4 consisted of the following 10 points:

- Set of 4 ICPs from the Cartosat-2 project RMSEx = 0.90m; RMSEy = 0.76m (G7001, G7010, G7012, G7023,);
- Set of 6 ICPs chosen and measured on the aerial ADS40 ortho: RMSEx = 0.90m; RMSEy = 0.76m (990064, 990065, 990067, 990069, 990070, 990079);

The projection and datum details of the above listed data are UTM zone 31N ellipsoid WGS84.

3. Methodology

3.1. Methodology overview

The EU standard for the orthoimagery to be used for the purpose of the Common Agriculture Policy (CAP) Control with Remote Sensing (CwRS) requires the quality assessment of the final orthoimage ('Guidelines …,' 2008).

The RMS error calculated for Independent Control Points (i.e. points not included in the sensor model parameter estimation process, derived from an independent source of higher accuracy) in each dimension (either Easting or Northing) is used to describe the geometric characteristics of the orthoimage (product accuracy). This procedure is often referred as to external quality control (EQC).

Our workflow consisted of the following phases:

(a) geometric correction model phase, also referred as to image correction phase, sensor orientation phase, space resection or bundle adjustment phase;

(b) orthocorrection - elimination of the terrain and relief related distortions through the use of sensor and terrain (elevation) information, then reprojection and resampling;

(c) external quality control (EQC) of the final product, also referred as to absolute accuracy check or validation phase.

During the image correction phase the following mathematical models were introduced to model the tested Kompsat-2 Standard SystemCorrected image:

- Rational Functions model (RPC) by PCI Geomatics 10.3.0, OrthoEngine module;
- Toutin's Rigorous model by PCI Geomatics 10.3.0, OrthoEngine module.
- Rational Functions model (RPC) by ERDAS LPS ver10.1;

While using the RPC method, polynomial order was set to 0 or 1.

The planimetric accuracy of orthoimage is quite sensitive to the number and distribution of the several ground control points (GCPs) used during image correction phase and orthorectification. Therefore, we studied several ground control points (GCPs) configurations, while the set of the independent check points (ICPs) remained unchanged for all tested variants. Each time, the 1-D RMS errors, for both X and Y directions were calculated for GCPs during the geometric correction model phase, and for ICPs – during the validation phase (EQC).

3.2. Kompsat-2 Sensor Support

At the time of Kompast-2 testing the current ERDAS Imagine and LPS version was 10.1. This version supports Kompsat-2 sensor by providing the RPC-based model, however it does not support the rigorous model for Kompsat-2. On the special request of authors, the ERDAS software developers created an enhancement request to add the Kompsat-2 model in the further versions of ERDAS Imagine and LPS.

The PCI Geomatics version 10.3.0 supports both the rigorous (Toutin's) and RPC-based Kompsat-2 sensor model.

3.3. Tested variants

We analysed geometric characteristics of the provided Kompsat-2 image depending on the number and distribution of the ground control points, i.e. points used for image correction and

orthorectification. The name of the variant (arrangement) includes the number that corresponds to the number of the GCPs used for geometric correction (compare Tab.3-6).

For all variants (GCPs configurations), we tried to keep the set of the independent check points unchanged (compare Figures 2-5).

Variant name	Number of GCP	GCPs distribution	List of GCPs	Number of ICPs
V_6	6	good	110008, G7001, 990045, 990046, 990047, 990052	15
V_9	9	good	110008, 440008, G7001, 66035, 990045, 990046, 990047, 990052, 990053	15
V_12	12	good	110008, 440008, G7001, 66035, 990045, 990046, 990047, 990050, 990051, 990052, 990053, 990054	15
V_15	15	good	110002,110008, 440008, G7001, 66035, 990045, 990046, 990047, 990048, 990049, 990050, 990051, 990052, 990053, 990054	15

Table 3: The list of tested variants characterised by different GCPs number and distribution over Kompsat-2 ID1 (geometric correction model phase)

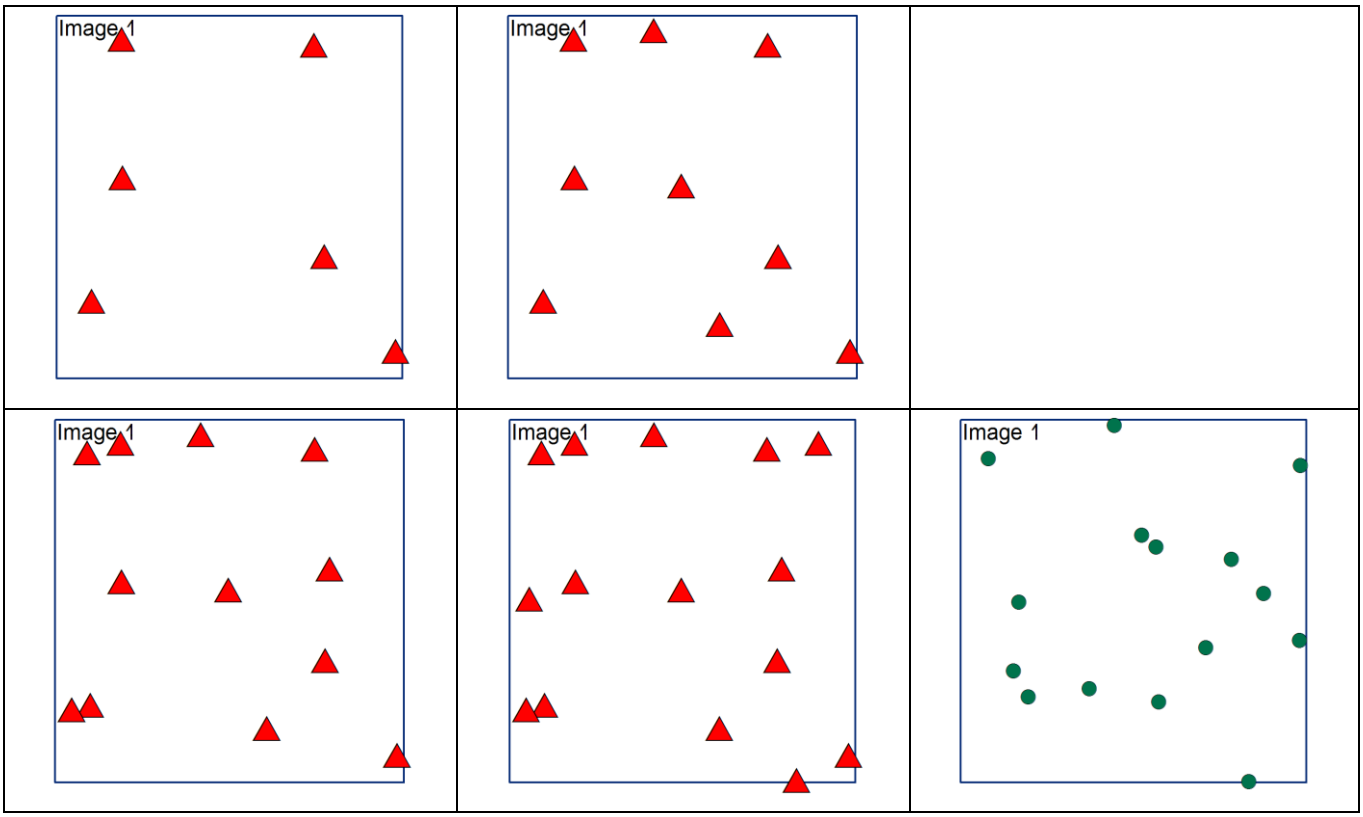

Figure 2: All tested variants (GCPs configurations) for ID1 Kompsat-2 image: in red - the variants with 6, 9, 12 and 15 GCPs; in green - the unchanged set of the 15 independent check points.

Variant name	Number of GCP	GCPs distribution	List of GCPs	Number of ICPs
V_6	6	good	110038, 990037, 990039, 990041, 990042, 990043	15
V_9	9	good	110038, 440008, G7001, 66035, 990037, 990039, 990041, 990042, 990043	15
V_12	12	good	110038, 440008, G7001, 66035, 990035, 990036, 990037, 990038, 990039, 990041, 990042, 990043	15
V_15	15	good	110008, 110038, 440008, G7001, 66035, 990026, 990035, 990036, 990037, 990038, 990039, 990040, 990041, 990042, 990043	15

Table 4: The list of tested variants characterised by different GCPs number and distribution over Kompsat-2 ID2 (geometric correction model phase)

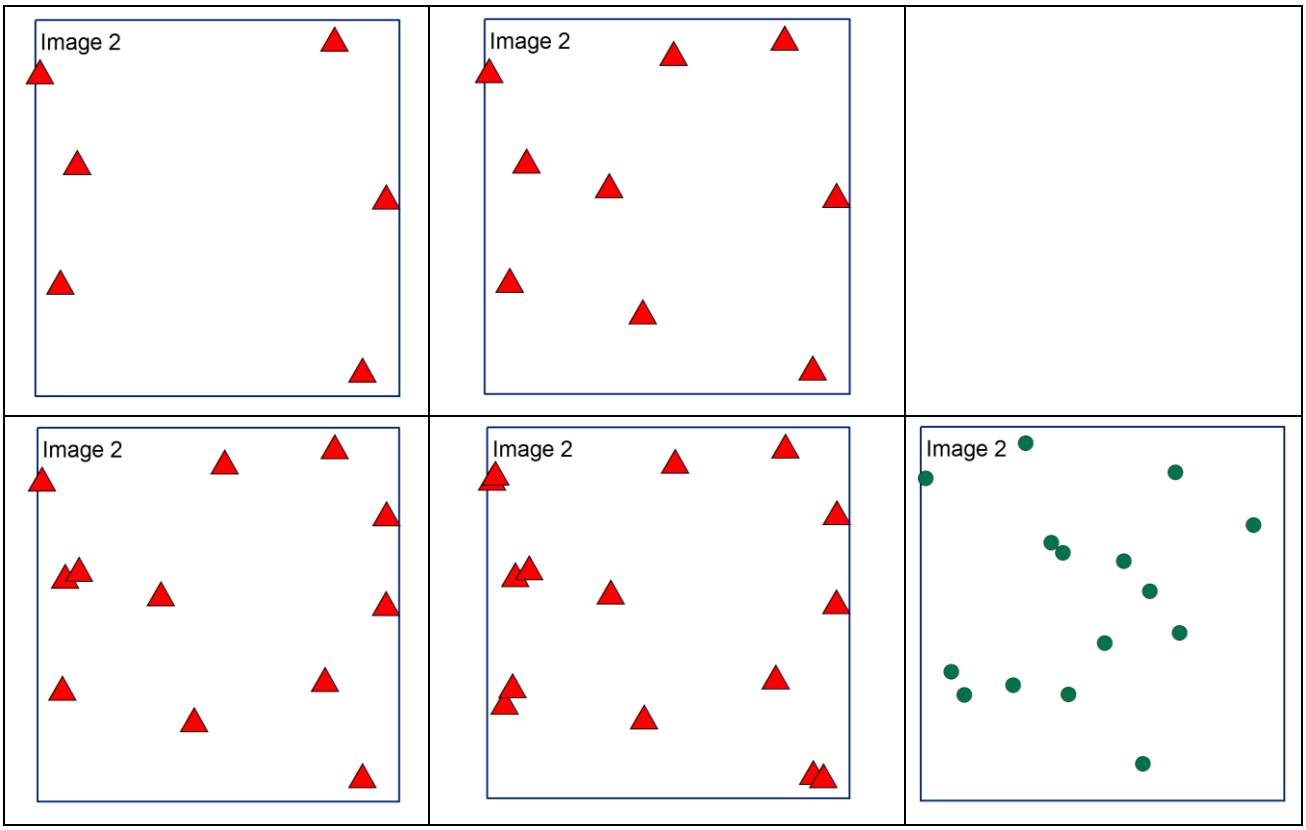

Figure 3: All tested variants (GCPs configurations) for ID2 Kompsat-2 image: in red - the variants with 6, 9, 12 and 15 GCPs; in green - the unchanged set of the 15 independent check points.

Variant name	Number of GCP	GCPs distribution	List of GCPs	Number of ICPs
V_6	6	good	990054, 990055, 990057, 990058, 990059, 990060	10
V_9	9	good	990049, 990054, 990055, 990056, 990057, 990058, 990059, 990060, 990063	10
V_12	12	good	990049, 990054, 990055, 990056, 990057, 990058, 990059, 990060, 990061, 990062, 990063, 990064	10

Table 5: The list of tested variants characterised by different GCPs number and distribution over Kompsat-2 ID3 (geometric correction model phase)

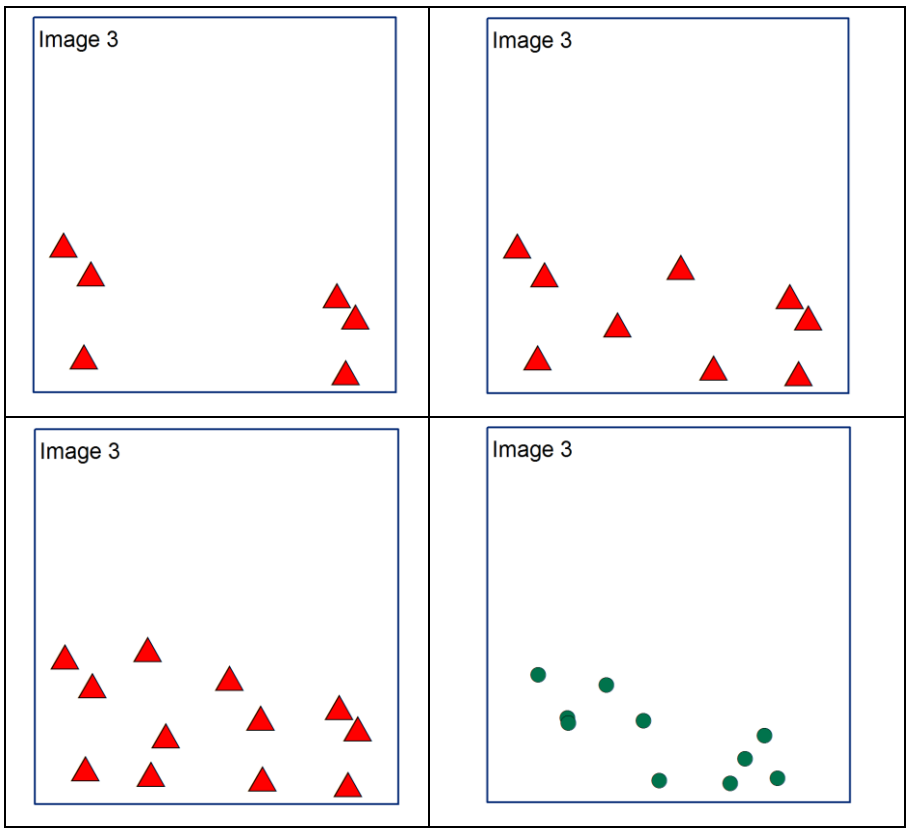

Figure 4: All tested variants (GCPs configurations) for ID3 Kompsat-2 image: in red - the variants with 6, 9 and 12 GCPs; in green - the unchanged set of the 10 independent check points.

Variant name	Number of GCP	GCPs distribution	List of GCPs	Number of ICPs
V_6	6	good	990008, 990057, 990073, 990075, 990076, 990080	10
V_9	9	good	G7003, 990008, 990049, 990057, 990072, 990073, 990075, 990076, 990080	10
V_12	12	good	G7003, 990008, 990049, 990056, 990057, 990058, 990062, 990072, 990073, 990075, 990076, 990080	10

Table 6: The list of tested variants characterised by different GCPs number and distribution over Kompsat-2 ID4 (geometric correction model phase)

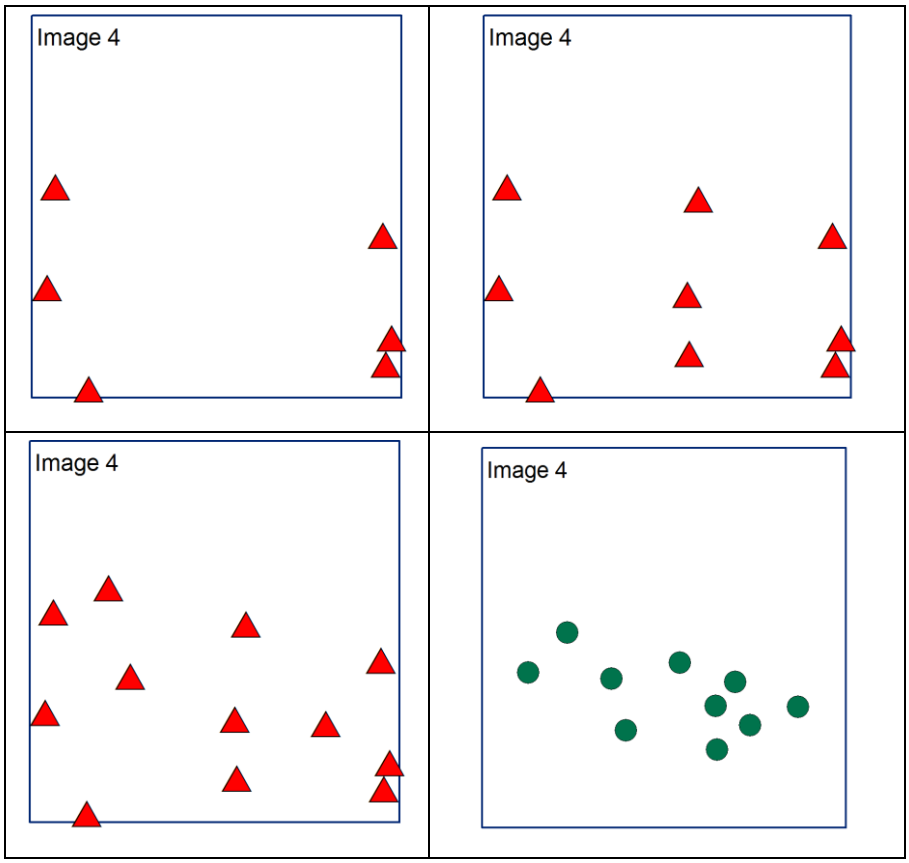

Figure 4: All tested variants (GCPs configurations) for ID4 Kompsat-2 image: in red - the variants with 6, 9 and 12 GCPs; in green - the unchanged set of the 10 independent check points.

3.4. Untested variants

There are some variants that have not been tested. In particular, the ID3 image was not tested using PCI Geomatics software due to a specific software limitation.
The ID3 image and the DTM data overlap only in 30%. Surprisingly this is too small overlap for PCI Geomatics to perform orthorectification process.

4. Results

4.1. Image correction results – RPC model by PCI Geomatics

Applying the model based on provided RPC parameters and setting the polynomial degree to one, we obtain the following RMSE results summarised in the Table 7-8.

			Img ID1		**Img ID2**	
			GCPs		**GCPs**	
Variant name	Number of GCPs	RPC order	**RMSE_X [m] Easting**	**RMSE_Y [m] Northing**	**RMSE_X [m] Easting**	**RMSE_Y [m] Northing**
V_6	**6**	**1**	**1.09**	**2.66**	**1.06**	**2.68**
V_9	**9**	**1**	**1.06**	**2.05**	**0.97**	**2.05**
V_12	**12**	**1**	**1.27**	**1.61**	**0.85**	**1.76**
V_15	**15**	**1**	**1.52**	**1.40**	**0.72**	**1.43**
V_6	**6**	**0**	**1.47**	**2.30**	**1.80**	**2.54**
V_9	**9**	**0**	**1.24**	**1.87**	**1.61**	**2.13**
V_12	**12**	**0**	**1.37**	**1.91**	**1.44**	**2.30**
V_15	**15**	**0**	**1.55**	**2.14**	**1.45**	**2.51**

Table 7: The 1-D RMS errors obtained for img 1&2 during the geometric correction model phase (RPC method) for different GCPs number and distribution while the number and distribution of the ICPs is constant, and so is the rational function order.

			Img ID3		**Img ID4**	
			GCPs		**GCPs**	
Variant name	Number of GCPs	RPC order	**RMSE_X [m] Easting**	**RMSE_Y [m] Northing**	**RMSE_X [m] Easting**	**RMSE_Y [m] Northing**
V_6	6	1	**-**	**-**	**0.47**	**1.71**
V_9	9	1	**-**	**-**	**0.47**	**1.42**
V_12	12	1	**-**	**-**	**1.00**	**2.83**
V_15	15	1	**-**	**-**		**-**
V_6	6	0	**-**	**-**	**1.01**	**7.83**
V_9	9	0	**-**	**-**	**0.92**	**6.42**
V_12	12	0	**-**	**-**	**1.40**	**5.97**
V_15	15	0	**-**	**-**	**-**	**-**

Table 8: The 1-D RMS errors obtained for img 3&4 during the geometric correction model phase (RPC method) for different GCPs number and distribution while the number and distribution of the ICPs is constant, and so is the rational function order.

4.2. Outcome of the external quality control for RPC model by PCI Geomatics

We performed the external quality control on each of the orthoimage produced for each image correction variant of the Kompsat-2 image ID1. The number and distribution of the ICPs is constant (thirteen-point data set). The result are summarised in the Tab.9-10 for not variable RPC polynomial order (introduced during previous, i.e. image correction, phase).

				Img ID1		**Img ID2**	
				ICPs		**ICPs**	
Variant name	Number of GCPs	Number of ICPs	RPC order	**RMSE_X [m] Easting**	**RMSE_Y [m] Northing**	**RMSE_X [m] Easting**	**RMSE_Y [m] Northing**
V_6	6	15	1	**1.98**	**6.63**	**2.34**	**4.63**
V_9	9	15	1	**2.16**	**6.09**	**2.32**	**4.38**
V_12	12	15	1	**2.64**	**5.79**	**2.44**	**4.26**
V_15	15	15	1	**2.74**	**5.55**	**2.50**	**3.74**
V_6	6	15	0	**2.86**	**6.09**	**2.96**	**4.99**
V_9	9	15	0	**2.68**	**5.87**	**3.25**	**4.91**
V_12	12	15	0	**2.92**	**6.19**	**3.11**	**4.72**
V_15	15	15	0	**2.85**	**6.11**	**3.04**	**4.82**

Table 9: The 1-D RMS errors obtained for img 1&2 during the external quality control. The number and distribution of the ICPs is constant (within one image).

				Img ID3		**Img ID4**	
				ICPs		**ICPs**	
Variant name	Number of GCPs	Number of ICPs	RPC order	**RMSE_X [m] Easting**	**RMSE_Y [m] Northing**	**RMSE_X [m] Easting**	**RMSE_Y [m] Northing**
V_6	6	10	1	**-**	**-**	**1.31**	**2.30**
V_9	9	10	1	**-**	**-**	**1.27**	**1.70**
V_12	12	10	1	**-**	**-**	**1.27**	**1.25**
V_15	15	10	1	**-**	**-**	**-**	**-**
V_6	6	10	0	**-**	**-**	**0.97**	**3.28**
V_9	9	10	0	**-**	**-**	**0.92**	**3.33**
V_12	12	10	0	**-**	**-**	**0.98**	**3.31**
V_15	15	10	1	**-**	**-**	**-**	**-**

Table 10: The 1-D RMS errors obtained for img 3&4 during the external quality control. The number and distribution of the ICPs is constant (within one image).

4.3. Image correction results – Rigorous model by PCI Geomatics

Applying the Toutin's rigorous model, we obtained the following RMSE results summarised in the Tables 11-12.

		Img ID1		**Img ID2**	
		GCPs		**GCPs**	
Variant name	Number of GCPs	**RMSE_X [m] Easting**	**RMSE_Y [m] Northing**	**RMSE_X [m] Easting**	**RMSE_Y [m] Northing**
V_6	6	**0.00**	**0.00**	**0.07**	**0.00**
V_9	9	**0.59**	**0.79**	**0.22**	**0.29**
V_12	12	**1.05**	**0.69**	**0.20**	**0.71**
V_15	15	**1.06**	**0.65**	**0.28**	**0.69**

Table 11: The 1-D RMS errors obtained for img 1&2 during the geometric correction model phase using rigorous Toutin's model for different GCPs number and distribution while the number and distribution of the ICPs is constant.

		Img ID3		**Img ID4**	
		GCPs		**GCPs**	
Variant name	Number of GCPs	**RMSE_X [m] Easting**	**RMSE_Y [m] Northing**	**RMSE_X [m] Easting**	**RMSE_Y [m] Northing**
V_6	6	**-**	**-**	**0.05**	**0.03**
V_9	9	**-**	**-**	**0.35**	**0.21**
V_12	12	**-**	**-**	**0.97**	**2.50**
V_15	15	**-**	**-**	**-**	**-**

Table 12: The 1-D RMS errors obtained for img 3&4 during the geometric correction model phase using rigorous Toutin's model for different GCPs number and distribution while the number and distribution of the ICPs is constant.

4.4. Outcome of the external quality control for rigorous model by PCI Geomatics

We performed the external quality control on each of the orthoimage produced for each image correction variant using Toutin's rigorous model implemented in the PCI Geomatica 10.2. OrthoEngine. The number and distribution of the ICPs is constant.

		Img ID1		**Img ID2**	
		ICPs		**ICPs**	
Variant name	Number of GCPs	**RMSE_X [m] Easting**	**RMSE_Y [m] Northing**	**RMSE_X [m] Easting**	**RMSE_Y [m] Northing**
V_6	6	**4.84**	**27.78**	**3.03**	**3.71**
V_9	9	**1.92**	**4.58**	**2.65**	**3.51**
V_12	12	**2.26**	**4.58**	**2.77**	**3.87**
V_15	15	**2.07**	**4.64**	**2.80**	**3.92**

Table 13: The 1-D RMS errors obtained for img 1&2 during the external quality control of the orthoimages obtained after introducing the rigorous Toutin's model.

		Img ID3		Img ID4	
		ICPs		ICPs	
Variant name	Number of GCPs	**RMSE_X [m] Easting**	**RMSE_Y [m] Northing**	**RMSE_X [m] Easting**	**RMSE_Y [m] Northing**
V_6	6	**-**	**-**	**26.66**	**12.32**
V_9	9	**-**	**-**	**1.18**	**1.44**
V_12	12	**-**	**-**	**1.27**	**1.24**
V_15	15	**-**	**-**	**-**	**-**

Table 14: The 1-D RMS errors obtained for img 3&4 during the external quality control of the orthoimages obtained after introducing the rigorous Toutin's model.

After removing systematic error the RMSE_E and RMSE_N for ID1 and ID2 (variant with 6 GCPs) are as follows:

ID1	**RMSE_X [m] Easting**	**RMSE_Y [m] Northing**
before	4.8	27.8
after	4.8	22.8
ID4	**RMSE_X [m] Easting**	**RMSE_Y [m] Northing**
before	26.6	12.3
after	8.9	9.1

Table 15: The 1-D RMS errors obtained for img 1&2 during the external quality control of the orthoimages obtained after introducing the rigorous Toutin's model, and after systematic error removal.

4.5. Image correction results – RPC model by ERDAS LPS

Applying theK2 ERDAS model based on RPC and setting the polynomial degree to one or zero, we obtain the following RMSE results summarised in the Tables 16-17.

			Img ID1		**Img ID2**	
			GCPs		**GCPs**	
Variant name	Number of GCPs	RPC order	**RMSE_X [m] Easting**	**RMSE_Y [m] Northing**	**RMSE_X [m] Easting**	**RMSE_Y [m] Northing**
V_6	6	1	**0.62**	**0.93**	**0.54**	**0.79**
V_9	9	1	**0.84**	**1.00**	**0.73**	**0.87**
V_12	12	1	**1.18**	**0.96**	**0.68**	**0.95**
V_15	15	1	**1.46**	**0.94**	**0.62**	**0.91**
V_6	6	0	**1.39**	**1.96**	**1.75**	**2.17**
V_9	9	0	**1.20**	**1.69**	**1.60**	**1.94**
V_12	12	0	**1.34**	**1.80**	**1.43**	**2.20**
V_15	15	0	**1.54**	**2.08**	**1.44**	**2.45**

Table 16: The 1-D RMS errors obtained for img 1&2 during the geometric correction model phase (ERDAS RPC method) for different GCPs number and distribution while the number and distribution of the ICPs is constant.

			Img ID3		**Img ID4**	
			GCPs		**GCPs**	
Variant name	Number of GCPs	RPC order	**RMSE_X [m] Easting**	**RMSE_Y [m] Northing**	**RMSE_X [m] Easting**	**RMSE_Y [m] Northing**
V_6	6	1	**0.62**	**1.02**	**0.36**	**0.26**
V_9	9	1	**1.34**	**2.09**	**0.45**	**0.69**
V_12	12	1	**1.60**	**1.93**	**0.98**	**2.70**
V_15	15	1	**-**	**-**	**-**	**-**
V_6	6	0	**1.42**	**1.16**	**0.55**	**7.82**
V_9	9	0	**1.53**	**2.15**	**0.62**	**6.41**
V_12	12	0	**1.63**	**1.96**	**1.18**	**5.97**
V_15	15	0	**-**	**-**	**-**	**-**

Table 17: The 1-D RMS errors obtained for img 3&4 during the geometric correction model phase (ERDAS RPC method) for different GCPs number and distribution while the number and distribution of the ICPs is constant.

4.1. Outcome of the external quality control for RPC model by ERDAS LPS

We performed similar external quality control on each of the orthoimage produced for each image correction variant of the Kompsat-2 image ID1,2,3 and 4. The number and distribution of the ICPs is constant (within one image). The results are summarised in the Tab.18-19 for not variable RPC polynomial order (introduced during previous, i.e. image correction, phase).

				Img ID1		**Img ID2**	
				ICPs		**ICPs**	
Variant name	Number of GCPs	Number of ICPs	RPC order	**RMSE_X [m] Easting**	**RMSE_Y [m] Northing**	**RMSE_X [m] Easting**	**RMSE_Y [m] Northing**
V_6	6	15	1	**2.09**	**5.20**	**2.47**	**3.72**
V_9	9	15	1	**2.20**	**4.96**	**2.32**	**3.80**
V_12	12	15	1	**2.21**	**4.86**	**2.39**	**3.57**
V_15	15	15	1	**2.57**	**4.59**	**1.97**	**3.38**
V_6	6	15	0	**2.74**	**6.10**	**3.07**	**4.95**
V_9	9	15	0	**2.87**	**6.19**	**2.98**	**4.90**
V_12	12	15	0	**2.63**	**6.20**	**3.00**	**4.85**
V_15	15	15	0	**2.67**	**5.92**	**2.76**	**4.66**

Table 18: The 1-D RMS errors obtained for img 1&2 during the external quality control. The number and distribution of the ICPs is constant (within one image).

				Img ID3		**Img ID4**	
				ICPs		**ICPs**	
Variant name	Number of GCPs	Number of ICPs	RPC order	**RMSE_X [m] Easting**	**RMSE_Y [m] Northing**	**RMSE_X [m] Easting**	**RMSE_Y [m] Northing**
V_6	6	10	1	**1.85**	**2.63**	**1.31**	**2.30**
V_9	9	10	1	**1.70**	**1.75**	**1.27**	**1.70**
V_12	12	10	1	**1.47**	**1.73**	**1.27**	**1.24**
V_15	15	10	1	**-**	**-**	**-**	**-**
V_6	6	10	0	**1.08**	**2.60**	**0.97**	**3.28**
V_9	9	10	0	**1.27**	**1.75**	**0.92**	**3.33**
V_12	12	10	0	**1.29**	**1.62**	**0.98**	**3.31**
V_15	15	10	0	**-**	**-**	**-**	**-**

Table 19: The 1-D RMS errors obtained for img 3&4 during the external quality control. The number and distribution of the ICPs is constant (within one image).

5. Discussion

5.1. PCI Geomatics rigorous model summary

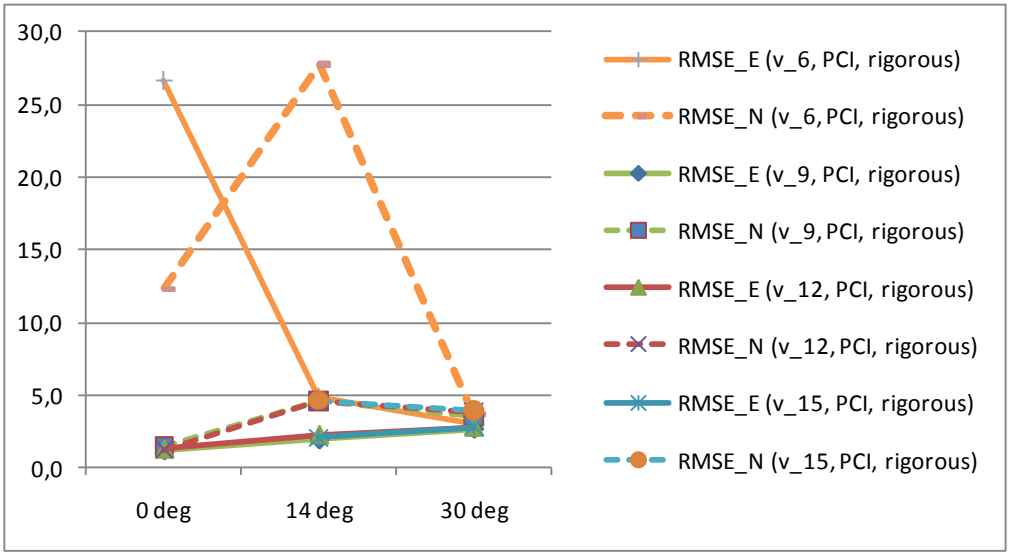

Figure 6: 1-D RMSE_ICP [m] measured on the final K2 orthoimage as a function of the overall off-nadir angle after the single scene correction applying the rigorous model (PCI Geomatics) based on 6, 9, 12 and 15 well-distributed GCPs and a DTM with 0.6m vertical accuracy.

Variant v_6 (6 GCPs) produced five times greater RMS errors than the RMS errors obtained for the variants v_9, v_12 and v_16. This strengthens the observation that rigorous sensor model should be used for scenes with more than six ground control points (fig.6).

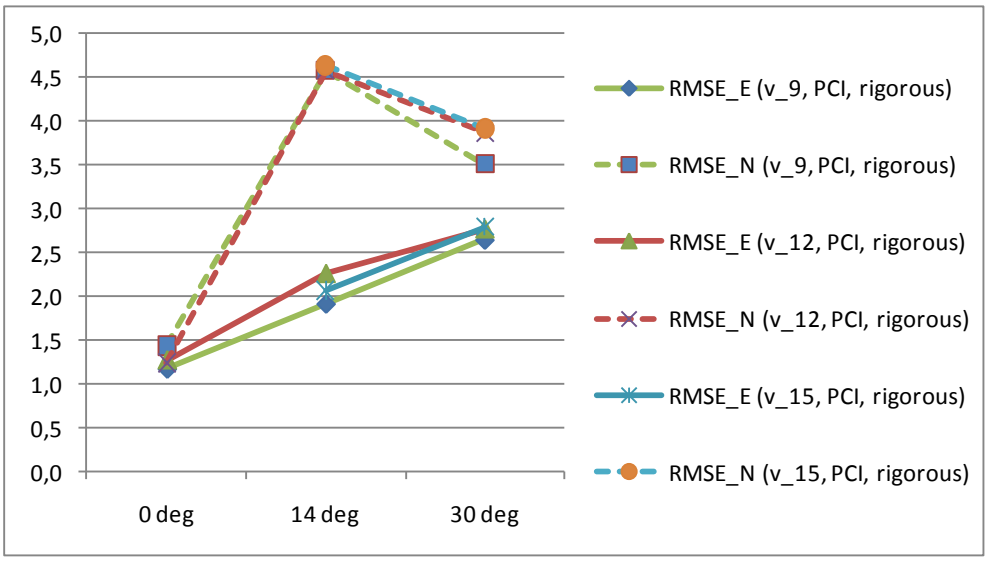

Figure 7: 1-D RMSE_ICP [m] measured on the final K2 orthoimage as a function of the overall off-nadir after the single scene correction applying the rigorous model (PCI Geomatics) based on 9, 12 and 15 well-distributed GCPs a DTM with 0.6m vertical accuracy.

The 1-D RMS errors measured on the final K2 orthoimage after the single scene correction applying the PCI rigorous model (fig.7):

- are not sensitive to the number of GCPs used if they are well-distributed and range between 9 and 15 (provided a DTM with 0.6m vertical accuracy)

- are sensitive to the overall off-nadir angle;

- increase with increasing off-nadir angle.

Note the lack of convergence with decreasing off-nadir angle for the RMS errors in the northing direction.

5.2. PCI Geomatics RPC-based model summary

The results of the four variants, i.e. 6, 9, 12 and 15 GCPs, are presented in figures 8-11. The 1-D RMSE_ICP measured on the final K2 orthoimage after the single scene correction applying first order Rational Polynomial are presented as solid lines, the zero-order Rational Polynomial RMSE results are presented as dotted lines. The 1-D RMSE_ICP results in the Easting direction are presented in green, while the results in the Northing direction are in red.

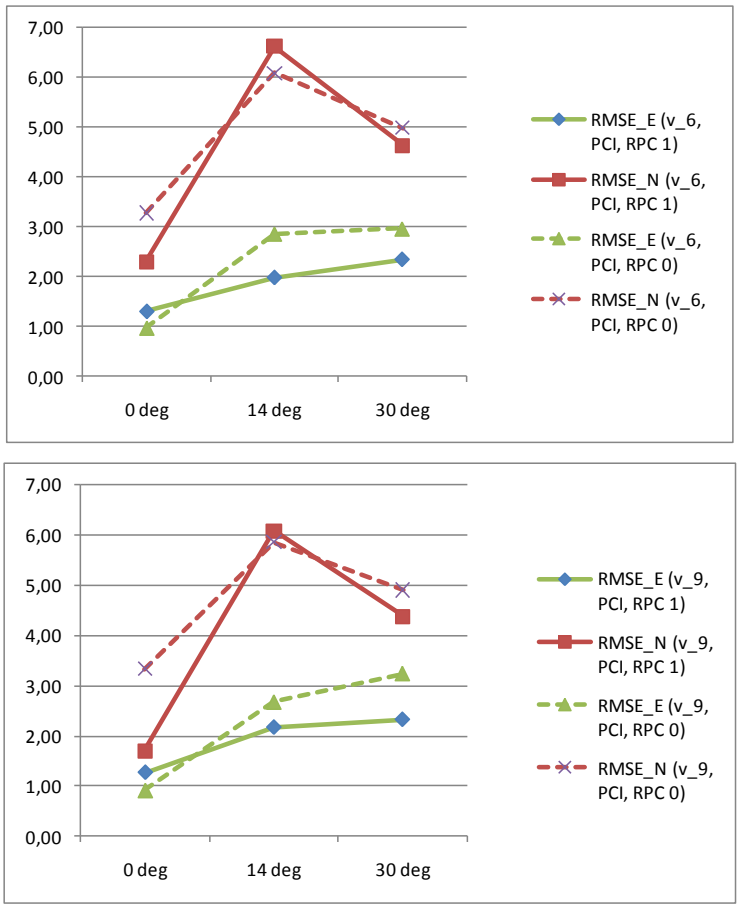

Figure 8, 9: 1-D RMSE_ICP [m] measured on the final K2 orthoimage as a function of the overall off-nadir angle after the single scene correction using RPC-based K2 sensor model (PCI Geomatics) based on 6 (above) and 9 (below) well-distributed GCPs and a DTM with 0.6m vertical accuracy.

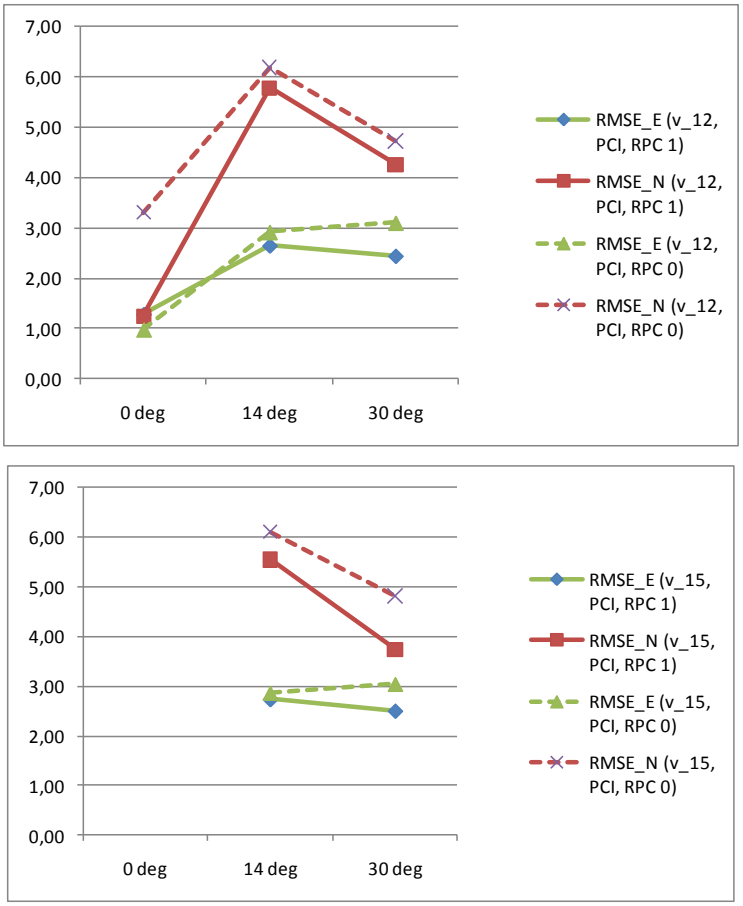

Figure 10, 11: 1-D RMSE_ICP [m] measured on the final K2 orthoimage as a function of the overall off-nadir angle after the single scene correction using RPC-based K2 sensor model (PCI Geomatics) based on 12 (above) and 15 (below) well-distributed GCPs and a DTM with 0.6m vertical accuracy.

The results of the four variants, i.e. 6, 9, 12 and 15 GCPs (PCI Geomatics), are presented in figures 12 and 13. Fig.12 shows the 1-D RMSE_ICP measured on the final K2 orthoimage after the single scene correction using first order Rational Polynomial and fig.13 shows the zero-order Rational Polynomial results. The 1-D RMSE_ICP in Easting direction are presented as solid lines, while the 1-D RMSE_ICP in Northing direction – as dotted ones.
Both approaches (zero and first order Rational Polynomial):

- are not sensitive to the number of GCPs used if they are well-distributed and range between 6 and 15, and particularly if they are more than 6 (provided a DTM with 0.6m vertical accuracy);
- are sensitive to the overall off-nadir angle;
- increase with increasing off-nadir angle.

Note the lack of convergence with decreasing off-nadir angle for the RMS errors in the northing direction (compare fig. 7, 12, 13).

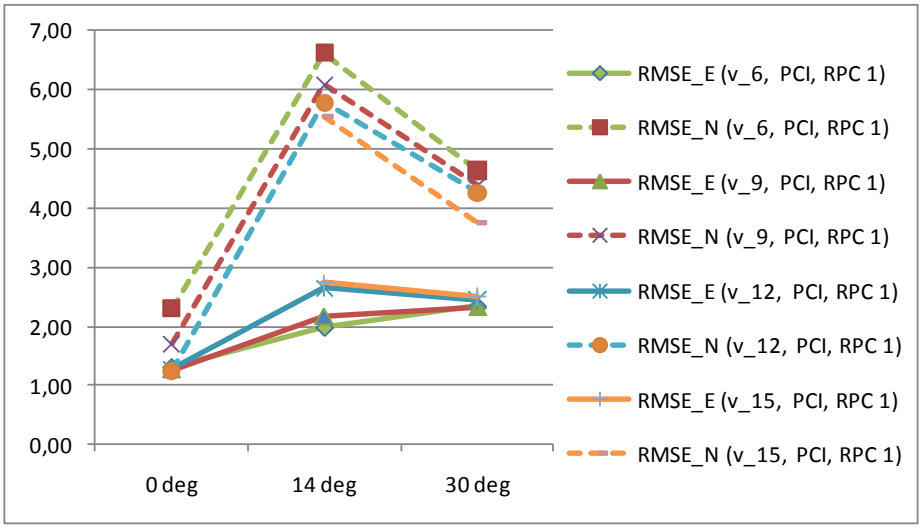

Figure 12: 1-D RMSE_ICP [m] measured on the final K2 orthoimage as a function of the overall off-nadir angle after the single scene correction applying the first order Rational Polynomial sensor model (PCI Geomatics) based on 6, 9, 12 and 15 well-distributed GCPs and a DTM with 0.6m vertical accuracy.

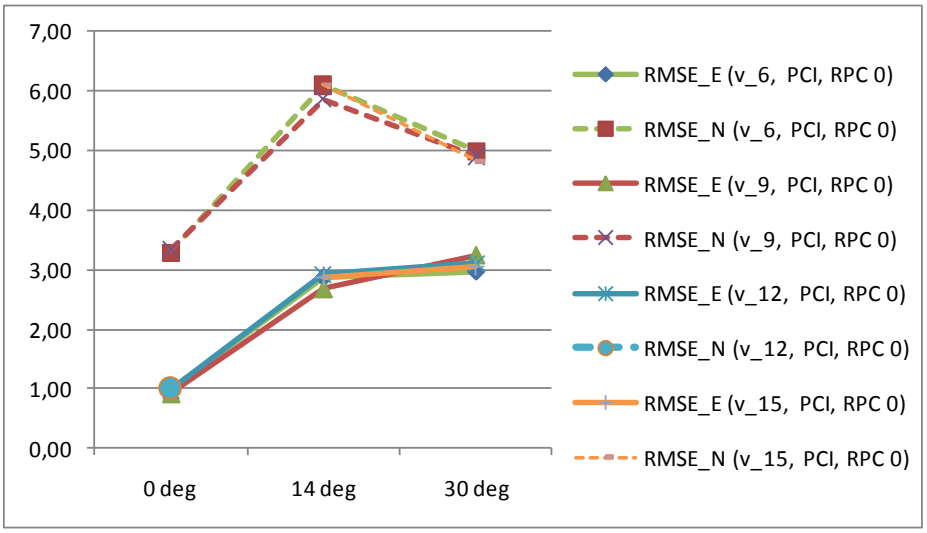

Figure 13: 1-D RMSE_ICP [m] measured on the final K2 orthoimage as a function of the overall off-nadir angle after the single scene correction applying the zero order Rational Polynomial sensor model (PCI Geomatics) based on 6, 9, 12 and 15 well-distributed GCPs and a DTM with 0.6m vertical accuracy.

5.3. PCI Geomatics RPC-based and rigorous models discussion

Figures 14 and 15 show the comparison between the 1-D RMSE_ICP [m] measured on the final K2 orthoimage as a function of the overall off-nadir angle after the single scene correction applying RPC-based (first and zero order respectively) K2 sensor model using PCI Geomatics (in red) and the PCI rigorous model (in green).
The average RMSE values are presented because of the similarity between the values obtained for variants with 9, 12 and 15 GCPs (compare fig. 7, 12, 13).

Comparing the K2 orthoimages produced using the PCI Geomatics RPC-based and rigorous models (fig.14, 15) present the following findings:

- The K2 orthoimage produced using the PCI rigorous model is characterised by smaller RMS errors (max 1 meter) than the K2 orthoimage produced using the PCI RPC-based model.
- The K2 orthoimage produced using the first order Rational Polynomial is characterised by RMS errors more similar to the rigorous model RMSE errors than the K2 orthoimage produced using the zero order Rational Polynomial.
- The RMSE values in the East direction (for rigorous and RPC-based models) are more similar each other than the RMSE values in North direction.
- The RMSE values for rigorous and RPC-based models are sensitive to the overall off-nadir angle and they increase with increasing off-nadir angle.

Note the lack of convergence with decreasing off-nadir angle for the RMS errors in the northing direction (compare fig. 7, 14, 15).

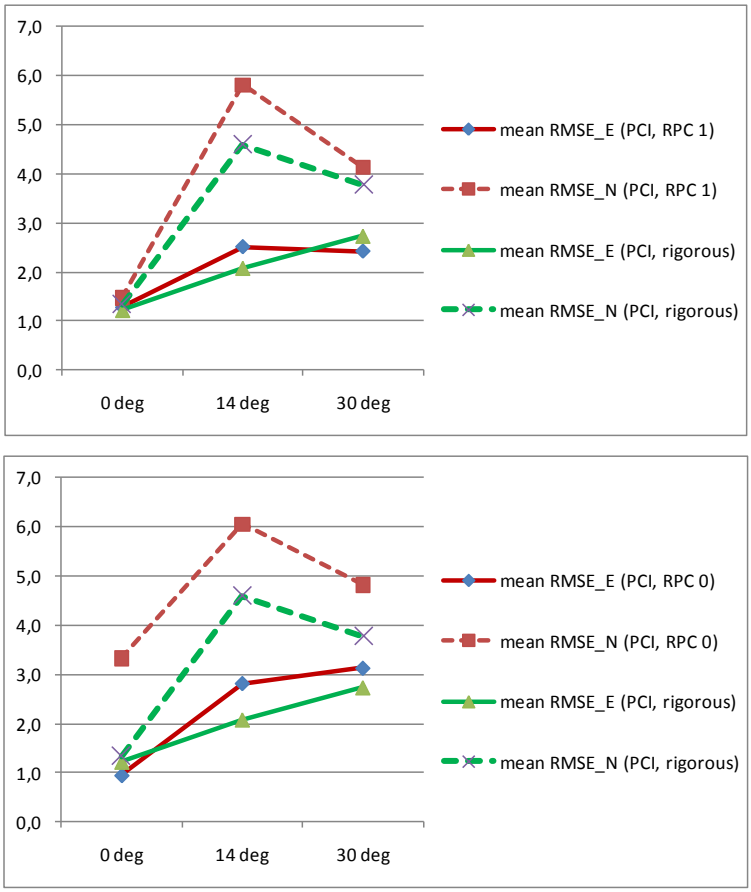

Figure 14, 15: The average 1-D RMSE_ICP [m] measured on the final K2 orthoimage as a function of the overall off-nadir angle after the single scene correction applying first (above) and zero (below) rational Polynomial sensor model using PCI Geomatics (in red) and by rigorous model using PCI Geomatics (in green).

5.4. ERDAS LPS RPC-based model summary

The results of the four variants, i.e. 6, 9, 12 and 15 GCPs (ERDAS LPS), are presented in figures 16-19. The 1-D RMSE_ICP measured on the final K2 orthoimage after the single scene correction applying first order Rational Polynomial are presented as solid lines, the zero-order Rational Polynomial RMSE results are presented as dotted lines. The 1-D RMSE_ICP results in the Easting direction are presented in green, while the results in the Northing direction are in red.

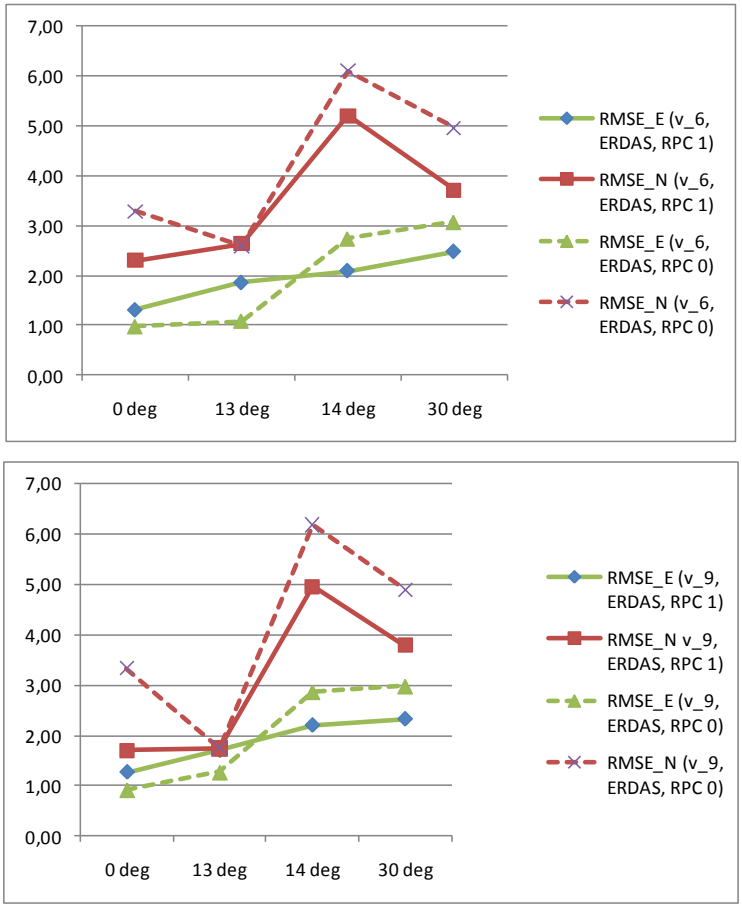

Figure 16, 17: 1-D RMSE_ICP [m] measured on the final K2 orthoimage as a function of the overall off-nadir angle after the single scene correction using RPC-based K2 sensor model (ERDAS LPS) based on 6 (above) and 9 (below) well-distributed GCPs and a DTM with 0.6m vertical accuracy.

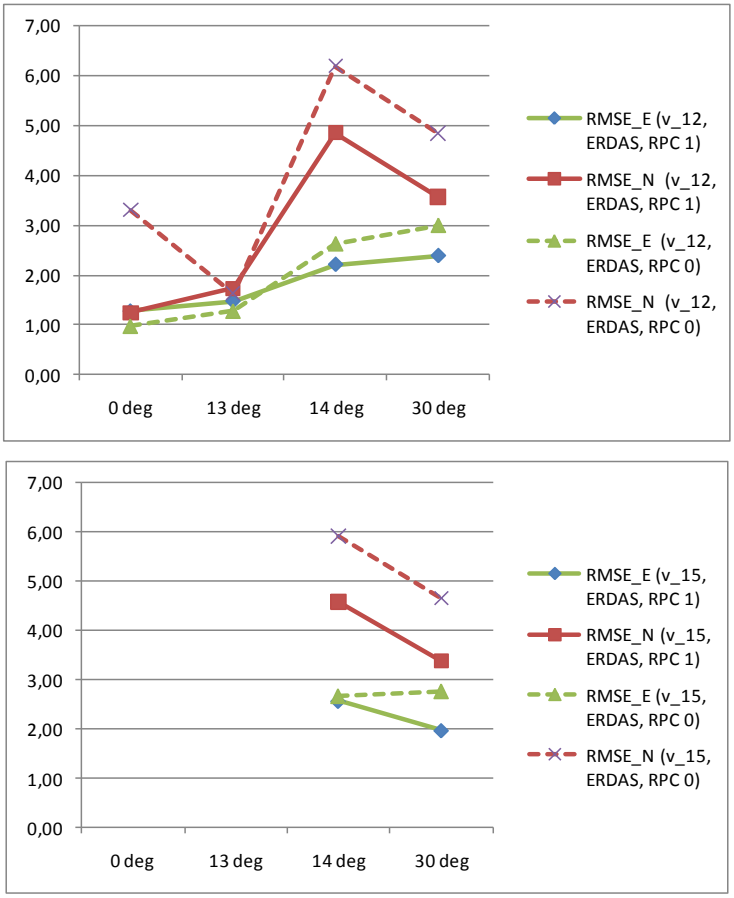

Figure 18, 19: 1-D RMSE_ICP [m] measured on the final K2 orthoimage as a function of the overall off-nadir angle after the single scene correction using RPC-based K2 sensor model (ERDAS LPS) based on 12 (above) and 15 (below) well-distributed GCPs and a DTM with 0.6m vertical accuracy.

The results of the four variants, i.e. 6, 9, 12 and 15 GCPs (ERDAS LPS), are presented in figures 20 and 21. Fig.20 shows the 1-D RMSE_ICP measured on the final K2 orthoimage after the single scene correction using first order Rational Polynomial and fig.21 shows the zero-order Rational Polynomial results. The 1-D RMSE_ICP in Easting direction are presented as solid lines, while the 1-D RMSE_ICP in Northing direction – as dotted ones.
Both approaches (zero and first order Rational Polynomial):

- are not sensitive to the number of GCPs used if they are well-distributed and range between 6 and 15, and particularly if they are more than 6 (provided a DTM with 0.6m vertical accuracy);
- are sensitive to the overall off-nadir angle;
- increase with increasing off-nadir angle.

Note the lack of convergence with decreasing off-nadir angle for the RMS errors in the northing direction (compare fig. 7, 20, 21).

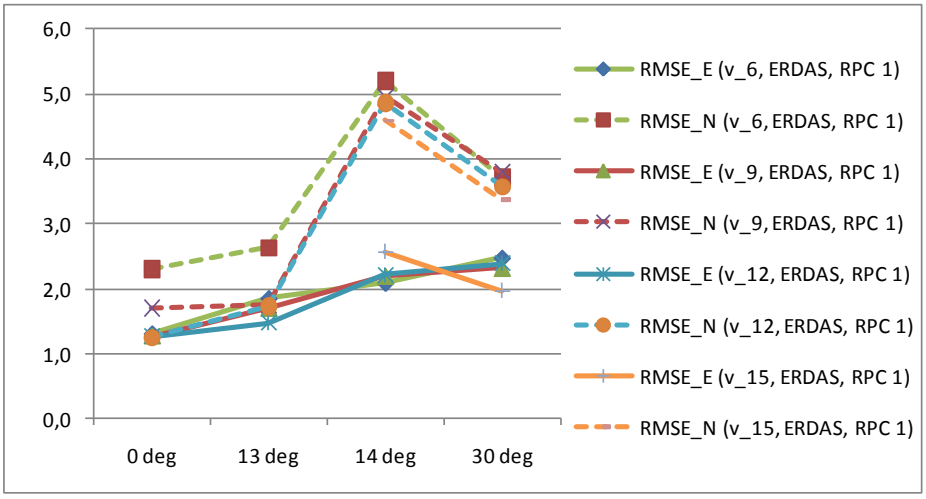

Figure 20: 1-D RMSE_ICP [m] measured on the final K2 orthoimage as a function of the overall off-nadir angle after the single scene correction by RPC-based first order K2 sensor model (using ERDAS LPS software) based on 6, 9, 12 and 15 well-distributed GCPs and 0.6m DTM accuracy.

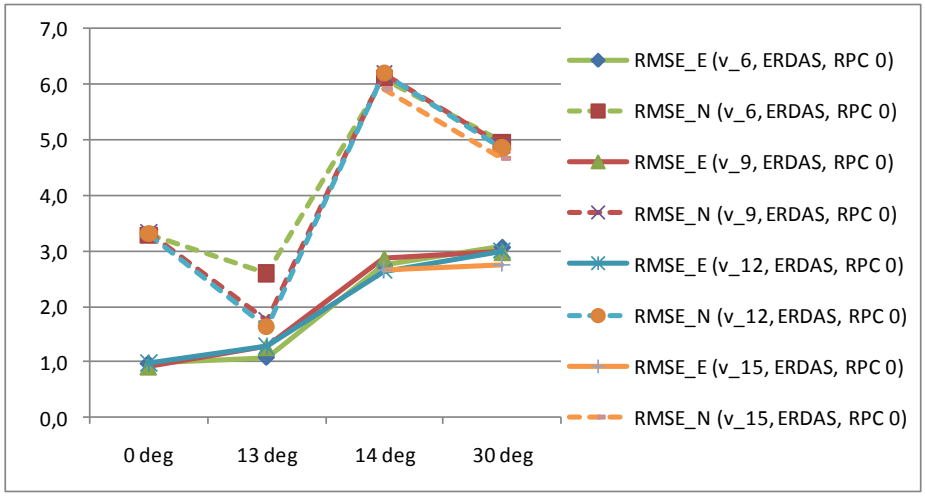

Figure 21: 1-D RMSE_ICP [m] measured on the final K2 orthoimage as a function of the overall off-nadir angle after the single scene correction by RPC-based zero-order K2 sensor model (using ERDAS LPS software) based on 6, 9, 12 and 15 well-distributed GCPs and 0.6m DTM accuracy.

5.5. ERDAS LPS RPC-based model and PCI rigorous model discussion

Figures 22 and 23 show the comparison between the 1-D RMSE_ICP [m] measured on the final K2 orthoimage as a function of the overall off-nadir angle after the single scene correction applying RPC-based (first and zero order respectively) K2 sensor model using ERDAS LPS (in red) and the PCI rigorous model (in green).
The average RMSE values are presented because of the similarity between the values obtained for variants with 9, 12 and 15 GCPs (compare fig. 7, 20, 21).

Comparing the K2 orthoimages produced using the ERDAS LPS RPC-based and PCI Geomatics rigorous models (fig.22, 23) present the following findings:

- The K2 orthoimage produced using the PCI rigorous model is characterised by smaller RMS errors (max 1 meter) than the K2 orthoimage produced using the ERDAS LPS RPC-based model.
- The K2 orthoimage produced using the ERDAS first order Rational Polynomial is characterised by RMS errors more similar to the PCI rigorous model RMSE errors than the K2 orthoimage produced using the zero order Rational Polynomial.
- The RMSE values in the East direction (for rigorous and RPC-based models) are more similar to each other than the RMSE values in North direction.
- The RMSE values for rigorous and RPC-based models are sensitive to the overall off-nadir angle and they increase with increasing off-nadir angle.

Note the lack of convergence with decreasing off-nadir angle for the RMS errors in the northing direction (compare fig. 7, 22, 23).

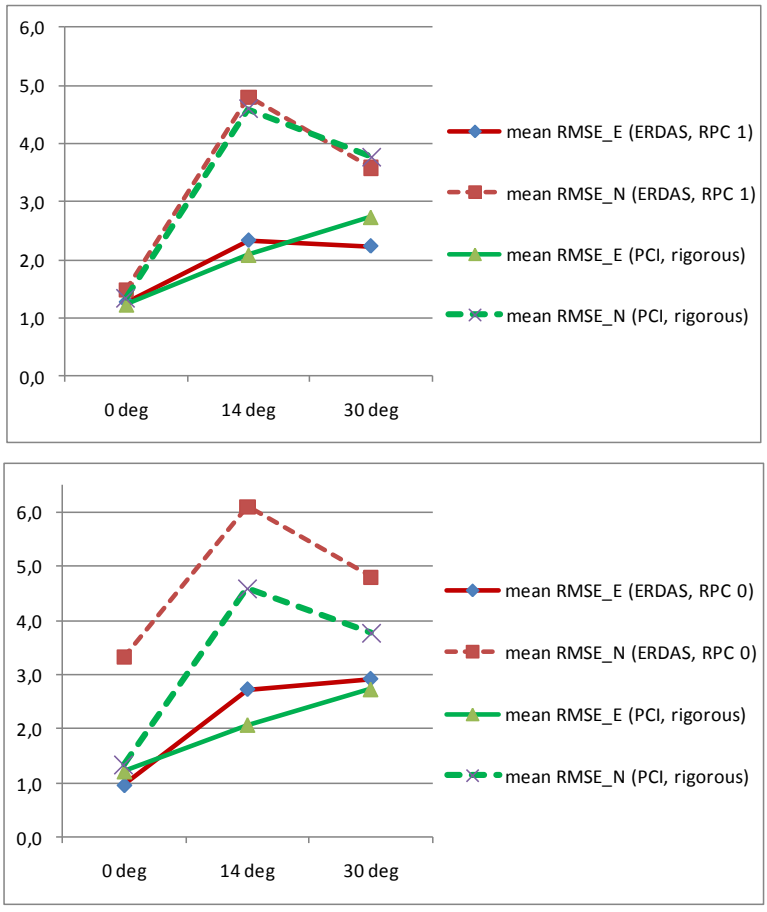

Figure 22, 23: The average 1-D RMSE_ICP [m] measured on the final K2 orthoimage as a function of the overall off-nadir angle after the single scene correction applying first (above) and zero (below) rational Polynomial sensor model using ERDAS LPS (in red) and by rigorous model using PCI Geomatics (in green).

5.6. ERDAS LPS RPC-based model and PCI Geomatics RPC-based model discussion

Figures 24 and 25 show the comparison between the 1-D RMSE_ICP [m] measured on the final K2 orthoimage as a function of the overall off-nadir angle after the single scene correction applying RPC-based (first and zero order respectively) K2 sensor model using ERDAS LPS (in blue) and the PCI RPC-based model (in red).
The average RMSE values are presented because of the similarity between the values obtained for variants with 9, 12 and 15 GCPs.

Comparing the K2 orthoimages produced using the ERDAS LPS RPC-based and PCI Geomatics RPC-based models (fig.24, 25) present the following findings:

- The K2 orthoimage produced using the ERDAS zero order Rational Polynomial is characterised by RMS errors very similar to the PCI zero order Rational Polynomial RMSE errors.
- The RMSE values in the East direction (for both models) are more similar to each other than the RMSE values in North direction.
- The RMSE values for rigorous and RPC-based models are sensitive to the overall off-nadir angle and they increase with increasing off-nadir angle.

Note the lack of convergence with decreasing off-nadir angle for the RMS errors in the northing direction (compare fig. 7, 24, 25).

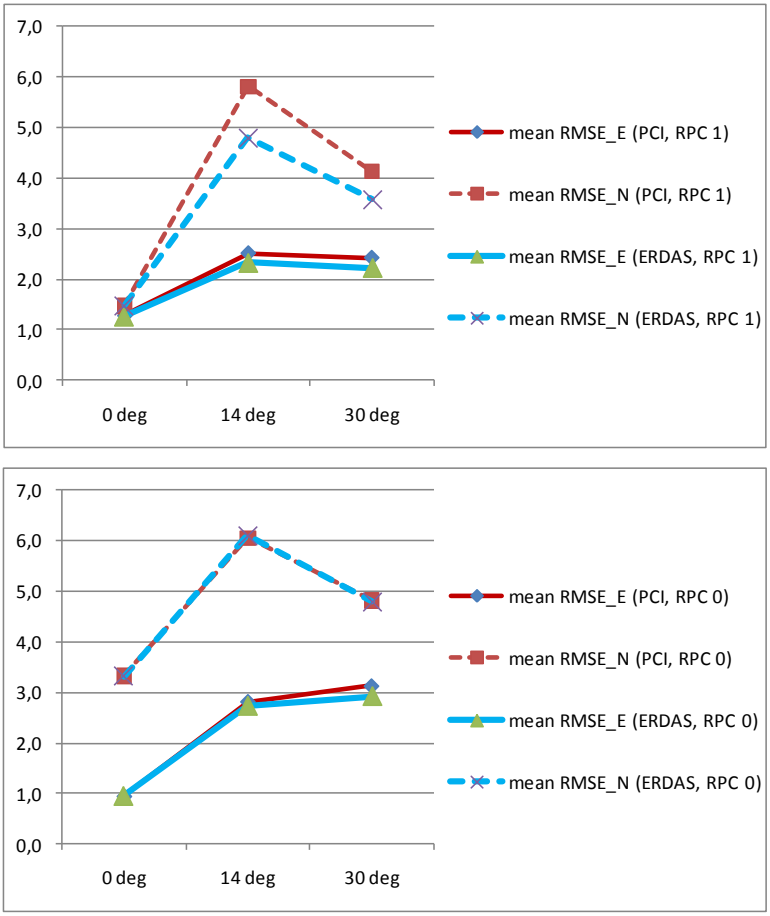

Figure 24, 25: The average 1-D RMSE_ICP [m] measured on the final K2 orthoimage as a function of the overall off-nadir angle after the single scene correction applying first order (above) and zero order (below) Rational Polynomial using ERDAS LPS (in blue) and PCI Geomatics (in red).

5.7. Average and maximum EQC results summary

			MAXIMUM		AVERAGE	
Model name	Software name	RPC order	**RMSE_X [m] Easting**	**RMSE_Y [m] Northing**	**RMSE_X [m] Easting**	**RMSE_Y [m] Northing**
Rational Polynomial	PCI Geomatics	1	**2.7**	**5.5**	**2.0**	**4.0**
	ERDAS LPS	1	**2.6**	**4.6**	**1.9**	**3.3**
Rational Polynomial	PCI Geomatics	0	3.2	6.2	2.3	4.7
	ERDAS LPS	0	3.0	6.2	2.2	4.7
Rigorous (Toutin's)	PCI Geomatics	n/a	**2.8**	**4.6**	**2.0**	**3.2**
overall			3.2	6.2	2.1	4.0

Table 20: The maximum and average values of the 1-D RMSE_ICP [m] measured on the final K2 orthoimage.

The K2 orthoimage produced using the PCI rigorous model is characterised by smaller RMS errors than the K2 orthoimage produced using the PCI/ERDAS RPC-based model, except where the imagery is characterised by an overall off-nadir angle close to zero degrees.

The K2 orthoimage produced using the first order Rational Polynomial is characterised by RMS errors more similar to the rigorous model RMSE errors than the K2 orthoimage produced using the zero order Rational Polynomial.

The K2 orthoimage produced using the ERDAS zero order Rational Polynomial is characterised by RMS errors very similar to the PCI zero order Rational Polynomial RMSE errors.

Both average (i.e. 2.1m and 4m) and maximum values (i.e. 3.2m and 6.2m) of the RMSE_E and RMSE_N are in line with the Saunier's (2008) Kompsat-2 Mission Quality Assessment. Moreover, these values are far better than the nominal horizontal geo-location accuracy of Kompsat-2 reported by Seo (2008), i.e. 2-D RMS error of 40.8m.

6. Summary of Key Issues

This report presents the geometric quality results recorded for the four samples of the Kompsat-2 radiometrically corrected images (processing level 1R) acquired over the JRC Maussane Terrestrial Test Site.

The key issues identified during the geometric quality testing based on the limited Kompsat-2 sample images that were made available to us are summarised below:

1. **The 1-D RMS errors** measured on the final K2 orthoimage after the single scene correction applying either the PCI rigorous model or the PCI RPC-based or the ERDAS RPC-based model:

- **are not sensitive to the number of GCPs** used if they are well-distributed and range between 9 and 15 (provided a DTM with 0.6m vertical accuracy);

- **are sensitive to the overall off-nadir angle** and increase with increasing off-nadir angle;

- in the Easting direction are more similar to each other than those in the Northing direction;

- in the Northing direction are characterised by the lack of convergence with decreasing off-nadir angle.

2. The 1-D RMS errors measured on the final K2 orthoimage after the single scene correction applying the PCI rigorous model based on six ground control points (GCPs):

- are five times greater than the RMS errors obtained for the variants with 9, 12 or 15 GCPs. This strengthens the observation that **rigorous sensor model should be used for scenes with more than six ground control points**.

3. Comparing the K2 orthoimages produced using the PCI Geomatics or ERDAS RPC-based model with the PCI rigorous models present the following findings:

- The K2 orthoimage produced using the PCI rigorous model is characterised by smaller RMS errors (max 1 meter) than the K2 orthoimage produced using the PCI/ERDAS RPC-based model.

- The K2 orthoimage produced using the first order Rational Polynomial is characterised by RMS errors more similar to the rigorous model RMSE errors than the K2 orthoimage produced using the zero order Rational Polynomial.

4. The K2 orthoimage produced using the ERDAS zero order Rational Polynomial is characterised by RMS errors very similar to the PCI zero order Rational Polynomial RMSE errors.

5. The average 1-D RMSE are 2.1m and 4m, while the maximum 1-D RMSE values are 3.2m and 6.2m of Easting and Northing direction respectively, provided a DTM with 0.6m vertical accuracy, and the GCPs with 0.05m < RMSEx, RMSEy < 0.90m are used.

6. **The orthorectified Kompsat-2 imagery do not fall within the accuracy criteria of the CwRS 1:10.000 scale requirements, i.e. an absolute 1-D RMSE of < 2.5m** (tab.20) except where the imagery is characterised by an overall off-nadir angle close to zero degrees and the rigorous model or first order Rational Polynomial sensor model is applied.

7. References

- Common Technical Specifications for the 2009 Campaign of Remote-Sensing Control of Area-Based Subsidies (ITT no. 2008/S 228-302473, JRC IPSC/G03/P/HKE/hke D(2008)(10021), Int. ref: file://S:\FMPArchive\P\10021.doc)
- Kapnias, D., Milenov, P., Kay, S., 2008. 'Guidelines for Best Practice and Quality Checking of Ortho Imagery' Issue 3.0. EUR 23638 EN – 2008, available on-line at: http://mars.jrc.ec.europa.eu/mars/Bulletins-Publications/Guidelines-for-Best-Practice-and-Quality-Checking-of-Ortho-Imagery-v-3.0 .
- Kay, S., Spruyt, P. and Alexandrou, K., 2003. Geometric quality assessment of orthorectified VHR space image data. Photogrammetric Engineering and Remote Sensing, 69, pp. 484-491.
- KOMPSAT-2 Image Data Manual (version 1.1., 2008-01-25)
- Nowak Da Costa, J.K., Tokarczyk, P.A., 2009. Maussane Test Site Auxiliary Data: Existing Datasets of the Ground Control Points. JRC Technical Report PUBSY no.JRC56257, IPSC/G03/C/JN/ D(2009)(11036), Int. ref: file://S:\FMPArchive\C\11036.pdf
- Nowak Da Costa, J.K., Tokarczyk, P.A., 2009. Kompsat-2: Initial findings of Geometric Image Quality Analysis. JRC Scientific and Technical Report PUBSY no.JRC56482, IPSC/G03/C/JNO/jno D(2009)(11233), Int. ref: file://S:\FMPArchive\C\11233.pdf
- Popova, S., Vassilev, V., 2008. Orthorectification of KOMPSat-2 as a Potential Source of Data for the CwRS Campaigns. MARS PAC Annual Conference presenation.
- Seo, D.C.[Doo Chun], Yang, J.Y.[Ji Yeon], Lee, D.H.[Dong Han], Song, J.H.[Jeong Heon], Lim, H.S.[Hyo Suk], 2008. KOMPSAT-2 Direct Sensor Modeling and Geometric Calibration/Validation. ISPRS Congress Beijing 2008, Proceedings of Commission I, available at: http://www.isprs.org/proceedings/XXXVII/congress/1_pdf/08.pdf
- Saunier, S., Collet, B., Mambimba, A., 2008. New Third Party Mission Quality Assessment. Kompsat-2 Mission. GAEL Consultant. Ref no. GAEL-P232-DOC-005. Available at: http://www.gael.fr/eoqc/pdf/GAEL-P232-DOC-005-01-02%20-%20Kompsat-2.pdf
- Ortho Product Testing – Kompsat-2 KARI/K2PS Accuracy Comparison, 2008. GAEL Consultant. Ref no. GAEL-P250-DOC-001. Available at: http://www.gael.fr/eoqc/pdf/GAEL-P250-DOC-003-01-03-OrthoProductValidation.pdf

European Commission

EUR 24542 EN – Joint Research Centre – Institute for the Protection and Security of the Citizen
Title: Geometric Quality Testing of the Kompsat-2 Image Data Acquired over the JRC Maussane Test Site using ERDAS LPS and PCI GEOMATICS remote sensing software
Author(s): Joanna Krystyna Nowak Da Costa, Agnieszka Walczyńska
Luxembourg: Publications Office of the European Union
2010 – 36 pp. – 29.7 x 21.0 cm
EUR – Scientific and Technical Research series – ISSN 1018-5593
ISBN 978-92-79-17007-2
doi:10.2788/21463

Abstract
This report presents the geometric quality results recorded for the four samples of the Kompsat-2 radiometrically corrected images (processing level 1R) acquired over the JRC Maussane Terrestrial Test Site. The objective of this study is threefold:

- to evaluate the planimetric accuracy in a routine basis production of orthorectified Kompsat-2 imagery;
- to determine the optimal number and spatial distribution of the GCPs (Ground Control Points) for the Kompsat-2 orthorectification process;
- to check if the orthorectified imagery of the Kompsat-2 optical sensor fall within the required accuracy criteria for the CwRS 1:10.000 scale of absolute 1-D RMSE of < 2.5m.

The key issues identified during the geometric quality testing based on the limited Kompsat-2 sample images that were made available to us are as follows:
1. The 1-D RMS errors measured on the final K2 orthoimage after the single scene correction applying either the PCI rigorous model or the PCI RPC-based or the ERDAS RPC-based model are not sensitive to the number of GCPs used if they are well-distributed and range between 9 and 15 (provided a DTM with 0.6m vertical accuracy); and are sensitive to the overall off-nadir angle and increase with increasing off-nadir angle.
2. The average 1-D RMSE are 2.1m and 4m, while the maximum 1-D RMSE values are 3.2m and 6.2m of Easting and Northing direction respectively, provided a DTM with 0.6m vertical accuracy, and the GCPs with 0.05m < RMSEx, RMSEy < 0.90m are used.
3. The orthorectified Kompsat-2 imagery do not fall within the accuracy criteria of the CwRS 1:10.000 scale requirements, i.e. an absolute 1-D RMSE of < 2.5m (tab.20) except where the imagery is characterised by an overall off-nadir angle close to zero degrees and the rigorous model or first order Rational Polynomial sensor model is applied.

How to obtain EU publications

Our priced publications are available from EU Bookshop (http://bookshop.europa.eu), where you can place an order with the sales agent of your choice.

The Publications Office has a worldwide network of sales agents. You can obtain their contact details by sending a fax to (352) 29 29-42758.

The mission of the JRC is to provide customer-driven scientific and technical support for the conception, development, implementation and monitoring of EU policies. As a service of the European Commission, the JRC functions as a reference centre of science and technology for the Union. Close to the policy-making process, it serves the common interest of the Member States, while being independent of special interests, whether private or national.

JRC
EUROPEAN COMMISSION

LB-NA-24542-EN-N

Publications Office

ISBN 978-92-79-17007-2